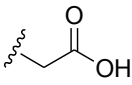
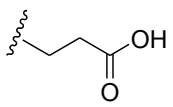
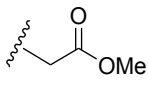


Supplemental Table 1. Structures and IC₅₀ of selected class A analogs.

Compound (DRA _{inh} -XX)	R ¹	R ²	IC ₅₀ (μM)
A250	3-Br-benzyl		0.15
A254	3-Cl-benzyl		0.20
A259	3-Me-benzyl		0.48
A256	2-F-benzyl		0.51
A255	3,5-Dimethyl-benzyl		0.54
A236	3-F-benzyl		0.84
A257	3,4-Dichloro-benzyl		1.8
A598	4- <i>tert</i> -Butyl-benzyl		4.6
A112	2,5-Dimethyl-benzyl		4.7
A129	Benzyl		5.1
A970	1-(2-methyl-naphthalene)-methylene-		inactive
A125	4-F-benzyl		inactive
A617	4- <i>tert</i> -Butyl-benzyl		inactive
A549	3-Methoxy-benzyl		inactive

Supplemental Table 2. Structures and IC₅₀ of selected class B analogs.

Compound (DRA _{inh} -XXX)	R ¹	R ²	IC ₅₀ (μM)
B601	Phenyl	3-Cl,4-Me-phenyl	1.5
B896	4-Cl-phenyl	4-Me-phenyl	1.6
B776	4-Ethoxy-phenyl	4-Cl-phenyl	1.7
B912	4-Cl-phenyl	4-Cl-phenyl	1.7
B895	4-Cl-phenyl	4-Br-phenyl	1.8
B739	4-Methoxy-phenyl	4-Br-phenyl	1.9
B695	3,5-Dimethyl-phenyl	3,4-Dichloro-phenyl	2.5
B689	3,5-Dimethyl-phenyl	3-Cl-4-Me-phenyl	2.1
B870	3-Cl-phenyl	4-Cl-phenyl	2.2
B835	4-F-phenyl	3,4-Dichloro-phenyl	2.6
B637	3-Cl-phenyl	3,4-Dichloro-phenyl	2.9
B656	2,3-Dimethyl-phenyl	4-Ethyl-phenyl	3.5
B685	3,5-Dimethyl-phenyl	4-Cl-phenyl	4.6
B716	3-Methoxy-phenyl	4-Cl-phenyl	4.7
B854	3-Cl-phenyl	4-Methyl-phenyl	5.1
B914	4-Cl-phenyl	4-Ethyl-phenyl	5.7
B629	3-Methyl-phenyl	4-Cl-phenyl	6.2
B614	3-Methyl-phenyl	4-Br-phenyl	6.4
B757	4-Methoxy-phenyl	4-Ethyl-phenyl	6.5
B740	3-Methoxy-phenyl	4-Methyl-phenyl	7.1
B911	4-Cl-phenyl	4-Nitro-phenyl	7.4
B917	4-Cl-phenyl	3-Cl,4-Me-phenyl	11
B920	4-Cl-phenyl	3-CF ₃ -Phenyl	12

SUPPLEMENTAL DETAILED METHODS

Molecular biology

Complementary DNA (cDNA) constructs for *slc26a3*, *SLC26A3*, *slc26a6*, and *slc26a9* were purchased from Origene (Rockville, MD). To generate *slc26a3* expression vector, a KpnI–EcoRI fragment excised from the Origene plasmid (containing the start codon and ~1.7 kb of the coding sequence) and a synthetic DNA fragment (gBLOCK, Integrated DNA Technologies (Coralville, IA), ~0.6 kb) encoding the carboxy-terminal *slc26a3* region, and 5'-EcoRI / 3'-BstXI/XhoI restriction sites, were used to regenerate *slc26a3* in pcDNA3.1/zeo(+) (Thermo Fisher Scientific, South San Francisco, CA). Subsequently, *slc26a3* cDNA, excised with BglII and BstXI, was subcloned into BamHI and BstXI sites of pIRESpuro3 (Clontech, Mountain View, CA). For *SLC26A3*, a KpnI-PstI fragment excised from the Origene plasmid (containing the start codon and ~1.9 kb of the coding sequence) and a ~0.6 kb gBLOCK encoding the carboxy-terminal *SLC26A3* region, and 5'-PstI and 3'-NotI restriction sites, were used to regenerate *SLC26A3* in pcDNA3.1/zeo(+). Subsequently, *SLC26A3* cDNA, excised with NheI and NotI, was subcloned into the SpeI and NotI sites of pLVX-IRES-mCherry (Clontech). To generate a plasmid for co-expression of *slc26a9* and halide sensitive EYFP-H148Q/I152L/F46L (YFP), pIRESpuro3 was digested with ApaI and XmaI and regenerated with a gBLOCK that replaced the puromycin resistance gene (Puro^r) with YFP, with the resultant vector termed pIRES-YFP. Subsequently, *slc26a9* was cloned into pIRES-YFP as an EcoRI-NotI fragment. To generate a lentiviral vector to co-express *slc26a6* and YFP, gBLOCKs were used to regenerate pLVX-Puro (Clontech) with YFP-T2A coding sequence inserted upstream of, and in frame with the Puro^r, with the resultant vector termed pLVX-YFP-T2A-Puro. A KpnI-PstI fragment was excised from the Origene *slc26a6* plasmid (containing ~2 kb of the 3'-region) and a ~0.5 kb gBLOCK encoding the amino-terminal *slc26a6* cDNA region with start codon, and 5'-NheI/EcoRI and 3'-KpnI restriction

sites, were used to regenerate slc26a6 in pcDNA3.1/zeo(+). Subsequently, full-length slc26a6 was subcloned into pLVX-YFP-T2A-Puro as an EcoRI to XbaI fragment. All constructs were confirmed by sequencing.

Cell culture and transfections

Fischer rat thyroid (FRT) cells were cultured in Kaign's modified Ham's F12 medium supplemented with 10 % FBS, 2 mM L-glutamine, 100 U/ml penicillin, 100 µg/ml streptomycin, 18 µg/ml myo-inositol and 45 µg/ml ascorbic acid, as described (1). For screening to identify slc26a3 inhibitors, FRT cells expressing YFP, generated using the FELIX third generation feline immunodeficiency lentiviral system available from Addgene (deposited by Garry Nolan, plasmid #1728) (1), were transfected with pIRESpuro3-slc26a3 using Lipofectamine 2000 (Thermo Fisher Scientific, South San Francisco, CA), selected using 0.15 mg/ml puromycin, and a clonal cell line (termed FRT-YFP-slc26a3) was isolated by functional assessment using a Cl⁻/I⁻-exchange protocol with YFP quenching as readout. FRT cells expressing YFP and slc26a4 (pendrin) or CFTR were previously described (2,3). HEK293T cells were cultured in DMEM containing 4.5 g/L glucose, 0.11 g/L sodium pyruvate, 0.584 g/L glutamine, 10 % FBS, 100 U/ml penicillin, and 100 µg/ml streptomycin, and transfected using NanoFect transfection reagent (Alstem, Richmond, CA) per manufacturer's instructions. To generate a cell line enriched for expression of SLC26A3, HEK293 cells were transduced with lentiviral particles generated with the pLVX-IRES-mCherry-SLC26A3 transfer vector. To generate a cell line enriched for expression of slc26a6 and YFP, HEK293 cells were infected with lentiviral particles generated with the pLVX-YFP-T2A-Puro-slc26a6 transfer vector, and selected with 0.2 mg/ml puromycin. Human immunodeficiency virus-based lentiviral particles were generated using standard procedures in HEK293 cells with the pMD2.G, pRSV-Rev, and pMDLg/pRRE packaging vectors available from Addgene (deposited by Didier Trono, plasmids #12251, #12253, and #12259).

Well-differentiated human bronchial epithelial (HBE) cells grown at an air-liquid interface were cultured as described (4).

Screening

High-throughput screening to identify slc26a3 inhibitors used a semi-automated Beckman Coulter (Indianapolis, IN) screening platform. FRT-YFP-slc26a3 cells were plated in 96-well black-walled, clear-bottom tissue culture plates (Corning Life Sciences, Tewksbury, MA) at a density of 20,000 cells/well and cultured for 48 hours until confluent. For screening, cells were washed twice in PBS and incubated for 10 min in 100 μ l PBS containing test compounds prior to assay of slc26a3 function. Screening was done on ~50,000 drug-like synthetic small molecules (ChemDiv, San Diego, CA) at a concentration of 25 μ M. Assays were done using a FLUOstar OMEGA plate reader (BMG Labtech, Cary, NC) over 12 s with initial fluorescence recorded over 1 s prior to addition of 100 μ l NaI-substituted PBS (137 mM NaCl replaced by 137 mM NaI) to drive Cl⁻/I⁻ exchange. The initial rate of Cl⁻/I⁻ exchange was determined from fluorescence intensity by single exponential regression. All plates contained wells with negative (1 % DMSO) and positive (350 μ M niflumic acid) controls. After initial screening, analogs of active compounds were purchased (ChemDiv) to generate structure-activity relationship data.

Compound selectivity

HEK293 cells transfected with pIRES-YFP-slc26a9 were plated in 96-well black-walled, clear-bottom tissue culture plates (Corning Life Sciences, Tewksbury, MA) after coating with FNC Coating Mix (AthenaES, Baltimore, MD). After washing two-times with PBS and incubating for 10 min in 100 μ l PBS containing 10 μ M DRA_{inh}-A250, cells were transferred to the stage of a TE2000 microscope (Nikon, Melville, NY) equipped with a C9100 EM-CCD (Hamamatsu, Campbell, CA),

Nikon 20× N.A. 0.75 S Fluor objective, and B-2E/C and 31002 filter sets (Chroma, Bellows Falls, VT) for imaging of green and red emitting fluorophores, respectively. Assays of slc26a9-mediated anion exchange were done by initially recording YFP fluorescence prior to addition of 100 µl of NaI-substituted PBS to test wells, with the initial rate of Cl⁻/I⁻ exchange deduced from fluorescence intensity by single exponential regression. Assays of slc26a6 activity were done in a similar manner using HEK cells transduced with lentiviral particles generated from the pLVX-YFP-T2A-Puro-slc26a6 vector. To assay SLC26A3 function, HEK293 cells transduced with lentiviral particles generated from the pLVX-IRES-mCherry-SLC26A3 transfer vector were transfected to express YFP for Cl⁻/I⁻ exchange assays as described above; red fluorescence images were acquired to confirm SLC26A3 expression in cells. CFTR function (3,5), pendrin-mediated Cl⁻/I⁻ exchange (2), and TMEM16A activity (6) were assayed as described. Short-circuit current (I_{sc}) measurements in well-differentiated HBE cell cultures were also done to assess compound selectivity. HBE cells were cultured at an air-liquid interface on Costar Snapwell clear permeable supports (12 mm diameter, 0.4 µm polyester membrane; Corning Life Sciences, Tewksbury, MA) and short-circuit current was measured using symmetrical HCO₃⁻-buffered solutions (in mM: 120 NaCl, 5 KCl, 1 MgCl₂, 1 CaCl₂, 5 Hepes, 25 NaHCO₃; pH 7.4; 95 % O₂ / 5 % CO₂ equilibration; 37 °C) with ion transport modulators added to both apical and basolateral bathing solutions as described (4).

Murine models

Animal experiments were approved by UCSF Institutional Animal Care and Use Committee (IACUC). Mice were housed in communal cages with standard rodent chow and water available ad libitum. Wild-type CD1 mice and ΔF508-CFTR homozygous mice were bred in the UCSF Laboratory Animal Resource Center.

Closed-loop studies

Female CD1 mice (age 8–10 weeks) were given free access to Pedialyte (per liter: Na⁺ 45 mEq, Cl⁻ 35 mEq, K⁺ 20 mEq, dextrose 25 g; Abbott, Abbot Park, IL) but not solid food for 48 h before experiments. Mice were treated with 500 μ L mineral oil once a day rectally (last dose 12 h before surgeries) during this period to evacuate the colon. Closed intestinal loops were isolated as described (7). Mice were anesthetized with isoflurane and body temperature was maintained during surgery at 36–38 °C using a heating pad. A small abdominal incision was made to expose the distal colon, and one closed distal colonic loop (length 1.5–2 cm) was isolated with sutures in each mouse. Loops were injected with 100 μ L phosphate-buffered saline (PBS, pH: 7.4, in mM: 137 NaCl, 2.7 KCl, 8 Na₂HPO₄, 1.8 KH₂PO₄, 1 CaCl₂, 0.5 MgCl₂) without and with 10 μ M DRA_{inh}-A250 and/or 10 μ M tenapanor (MedChemExpress, Monmouth Junction, NJ). The abdominal incision was closed with sutures, and mice were allowed to recover from anesthesia. Colonic loops were removed at 0 and 60 min (in separate mice) and loop length and weight were measured to quantify fluid absorption. Luminal fluid was emptied with a syringe and pH was measured immediately using AB15 pH Meter (Thermo Fisher Scientific, South San Francisco, CA). In separate studies, mid-jejunal loops (length 2-3 cm, 3–4 loops per mouse) were isolated as described above, injected with 100 μ L PBS without or with 10 μ M DRA_{inh}-A250 and/or 10 μ M tenapanor, and excised at 0 and 30 min to measure loop length and weight. In loop experiments, the final concentration of DMSO was 1% in vehicle, DRA_{inh}-A250 and/or tenapanor-treated loops.

To validate the closed-loop model as a method to quantify intestinal absorption (Figure S1), solutions containing 145 mM sodium chloride, 145 mM sodium gluconate, 145 mM choline chloride, or 110 mM glucose with 90 mM sodium chloride (all in distilled water with 1% DMSO) were prepared. The osmolality of the solutions, as measured by freezing-point depression osmometry (Precision Systems Inc, MA), and comparable (~290 mOsm/kg H₂O).

These solutions were injected to mid-jejunal loops (100 μ L) separately at 0 min and loops were excised at 30 min to quantify loop weight and length, as described above.

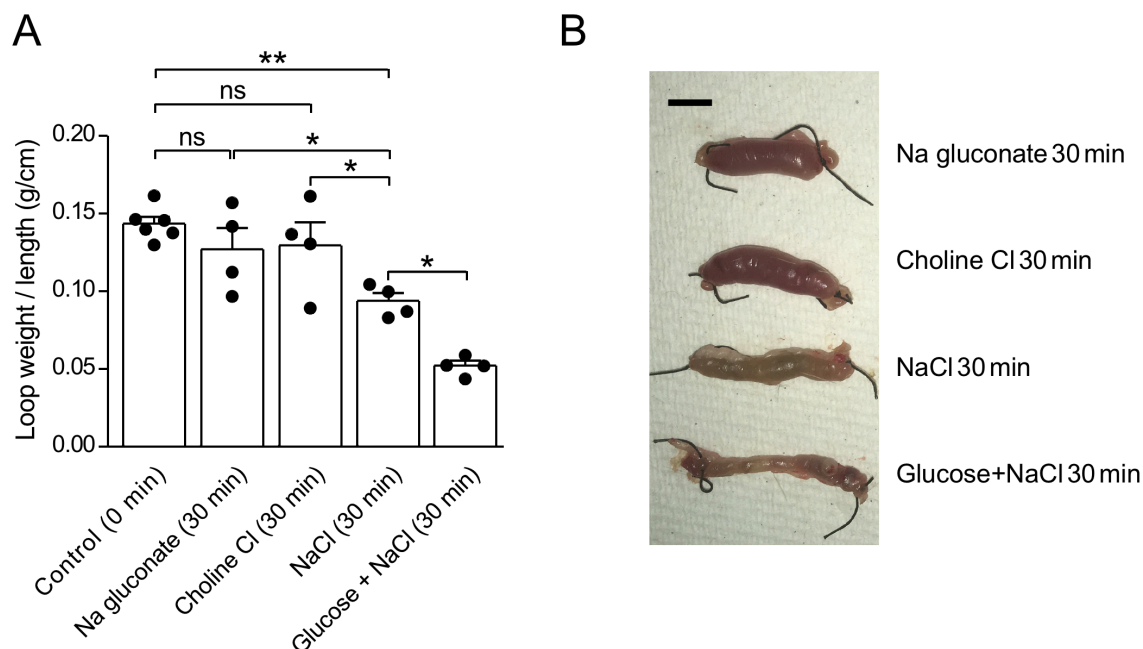


Figure S1. Validation of closed-loop model to study fluid absorption in the intestine. A. Loop weight/length ratio in mouse mid-jejunal closed loops (mean \pm S.E.M., n=4–6 loops per group). Fluid was absorbed (reduction in weight/length ratio) in jejunal sections injected with saline (NaCl), and largely inhibited by replacement of Na with the impermeant ion choline or replacement of Cl by gluconate. *P < 0.05, **P < 0.01, ns: not significant, one-way analysis of variance with post-hoc Newman-Keuls multiple comparisons test. B. Photos of representative excised jejunal loops injected with indicated solutions. Scale bar, 5 mm.

Loperamide-induced model of constipation

Female CD1 mice (age 8–10 weeks) were administered loperamide (0.3 mg/kg, intraperitoneally, in 5% Ethanol / 95 % PBS, 0.1 mg/mL final concentration, Sigma-Aldrich, St. Louis, MO) to produce constipation (3,8). DRA_{inh}-A250 (5 mg/kg, in saline containing vehicle (5% DMSO and 10% Kolliphor HS 15; Sigma-Aldrich)), tenapanor (5 mg/kg, in vehicle), both compounds (5 mg/kg each, in vehicle), or vehicle alone were administered by oral gavage 1 h before loperamide. The

final concentrations of DRA_{inh}-A250 and tenapanor were 0.5 mg/mL in vehicle. After loperamide injection, mice were placed individually in metabolic cages with *ad libitum* access to food and water. Stool samples were collected for 3 h, and total stool weight and number of fecal pellets were quantified. To measure stool water content, stool samples were dried at 80° C for 24 h and water content was calculated as [wet weight-dry weight]/wet weight. Similar studies were done in cystic fibrosis (CF) mice (Δ F508 homozygous) lacking functional CFTR.

Synthesis of DRA_{inh}-A250

All purchased materials and solvents were used without further purification. ¹H and ¹³C NMR spectra were determined on an Avance 300 MHz NMR Spectrometer (Bruker, San Jose, CA). Chemical shifts are given in parts per million (ppm). LC-MS analysis was performed using a Micromass ZQ Mass Spectrometer with 2695 HPLC Separations Module (Waters, Milford, MA). Compounds tested had >95% purity by LC/MS.

2-methylresorcinol (2.00 g, 16.09 mmol) and dimethyl 2-acetylsuccinate (3.03 g, 16.1 mmol) in absolute methanol (40 mL) were treated with dry HCl at 0 °C. The reaction mixture was then stirred at room temperature for 24 h, and the mixture was poured into water. The resulting precipitate was collected by filtration, washed with water, and dried to give an off-white solid (3.02 g, 72% yield) of the desired product (intermediate 1). ¹H NMR (300 MHz, MeOH-d₄) δ 7.51 (dd, J = 8.7, 0.45 Hz, 1H), 6.86 (d, J = 8.7 Hz, 1H), 3.728 (s, 2H), 3.720 (s, 3H), 2.41 (s, 3H), 2.27 (s, 3H); LC/MS m/z 262 (M + H⁺).

A mixture of 7-hydroxycoumarin (intermediate 1) (200 mg, 0.76 mmol), 3-bromobenzyl bromide (267 mg, 1.07 mmol), and potassium carbonate (211 mg, 1.53 mmol) in acetone (10 mL) was heated to reflux overnight. The solvent was evaporated and the residue poured into ice water. The resulting precipitate was collected by filtration, washed with methanol, and dried to give 290 mg (90%)

of coumarin ester (intermediate 2) as white solid. ^1H NMR (300 MHz, CDCl_3) δ 7.61 (brs, 1H), 7.51-7.48 (m, 1H), 7.46 (d, 1H, $J = 8.9$ Hz), 7.39 (d, 1H, $J = 8.0$ Hz), 7.29 (t, 1H, $J = 7.8$ Hz), 6.87 (d, 1H, $J = 8.9$ Hz), 3.75 (brs, 2H), 3.73 (s, 3H), 2.39 (brs, 6H); ^{13}C NMR (75 MHz, CDCl_3) δ 170.9, 161.8, 158.6, 151.6, 149.0, 138.8, 131.2, 130.2, 130.0, 125.5, 122.76, 122.72, 116.5, 114.5, 114.4, 108.1, 69.5, 52.2, 32.7, 15.3, 8.4; LC/MS m/z 431 ($\text{M} + \text{H}^+$).

To a solution of the ester intermediate 2 (180 mg, 0.42 mmol) in methanol (8 mL) was added NaOH (25 mg, 0.626 mmol) in water (2 mL) and the solution was heated to reflux for 1 h, cooled to room temperature, diluted with water and neutralized to pH 7.0 with 1N HCl. The resulting precipitate was collected by filtration, washed with water and dried to give DRA_{inh} -A250 as a white powder (105 mg, 60% yield). ^1H NMR (300 MHz, DMSO-d_6) δ 7.73 (brs, 1H), 7.66 (d, 1H, $J = 9.1$ Hz), 7.57-7.54 (m, 2H), 7.42-7.37 (m, 1H), 7.13 (d, 1H, $J = 8.9$ Hz), 5.34 (s, 2H), 3.73 (s, 2H), 2.45 (s, 3H), 2.33 (s, 3H); ^{13}C NMR (75 MHz, DMSO-d_6) δ 165.8, 161.4, 158.4, 151.1, 149.1, 144.1, 140.1, 131.2, 130.4, 126.7, 124.0, 122.2, 117.8, 114.4, 112.9, 109.2, 69.3, 33.6, 15.5, 8.5 ; LC/MS m/z 417 ($\text{M} + \text{H}^+$).

Cellular toxicity

T84 human colonic epithelial cells (provided by the UCSF Cell Culture facility) were cultured as previously described and seeded in black-walled, clear-bottom tissue culture plates (Corning Life Sciences, Tewksbury, MA) at a density of 20,000 cells/well (6). After 24 h culture, cells were treated with 10 μM DRA_{inh} -A250, 0.5 % DMSO (vehicle control) or 20 % DMSO (positive control) for an additional 24 hours prior to cytotoxicity assay using the AlamarBlue Cell Viability Reagent (ThermoFischer Scientific, Waltham, MA) according to the manufacturer's instructions (3). Data are presented as background-corrected normalized AlamarBlue fluorescence, with 0.5 % DMSO (vehicle) as control (normalized intensity of 1) (Figure S2).

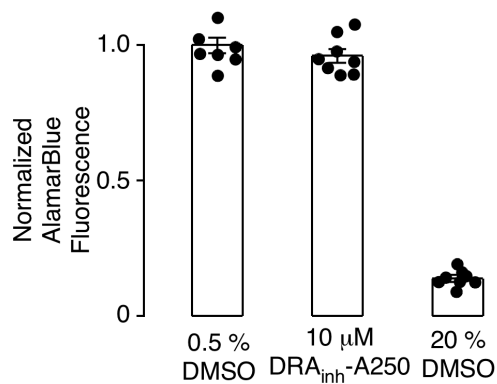


Figure S2. DRA_{inh}-A250 toxicity assay in T84 cells. Cells were treated with 10 μM DRA_{inh}-A250 or 0.5 % DMSO (vehicle control) or 20 % DMSO (positive control) for 24 h prior to AlamarBlue assay.

SUPPLEMENTAL REFERENCES

- 1 Haggie PM, et al. Correctors and potentiators rescue function of the truncated W1282X-cystic fibrosis transmembrane regulator (CFTR) translation product. *J Biol Chem.* 2017;292(3):771-85.
- 2 Cil O, Haggie PM, Phuan P-W, Tan JA, and Verkman AS. Small-molecule inhibitors of pendrin potentiate the diuretic action of furosemide. *J Am Soc Nephrol.* 2016;27(12):3706-14.
- 3 Cil O, et al. CFTR activator increases intestinal fluid secretion and normalizes stool output in a mouse model of constipation. *Cell Mol Gastroentrol.* 2016;2(3):317-27.
- 4 Haggie PM, et al. Inhibitors of pendrin anion exchange identified in a small molecule screen increase airway surface liquid volume in cystic fibrosis. *FASEB J.* 2016;30(6):2187-97.

- 5 Ma T, et al. Thiazolidinone CFTR inhibitor identified by high-throughput screening blocks cholera toxin-induced intestinal fluid secretion. *J Clin Invest.* 2002;110(11):1651-8.
- 6 Namkung W, Phuan P, and Verkman AS. TMEM16A inhibitors reveal TMEM16A as a minor component of CaCC conductance in airway and intestinal epithelial cells. *J Biol Chem.* 2011;286(3):2365-74.
- 7 Cil O, et al. Benzopyrimido-pyrrolo-oxazine-dione CFTR inhibitor (R)-BPO-27 for antisecretory therapy of diarrheas caused by bacterial enterotoxins. *FASEB J* 2017;31(2):751-60.
- 8 Cil O, et al. Phenylquinoxalinone CFTR activator as potential prosecretory therapy for constipation. *Transl Res.* 2016;182;14-26.e4.